American Journal of Science

MARCH 1940

STRUCTURAL PETROLOGY OF THE SCHISTS OF EASTERN OTAGO, NEW ZEALAND.

F. J. TURNER.

Part II.

The East Coastal Section.

ALONG the east coast of Otago for a distance of ten miles from the mouth of the Taieri River to just north of Brighton there are continuous outcrops of schist except where covered by local expanses of dune- or beach-sands. The rank of metamorphism increases northward in this section from Subzone Chl_2 to Chl_4 of the Chlorite Zone, and simultaneously the structure becomes increasingly complex as flat-lying or gently inclined slates and phyllonites grade northward into folded schists which in turn pass into rocks in which the presence of several distinct megascopic schistosities complicates the structure yet further. It is hoped later to examine this coastal section in much fuller detail, but for the purpose of this paper, work has been confined to a few representative rocks from a limited number of stations.

Specimen No. 4712

Locality: N side of mouth of Taieri River.
Schistosity (slaty cleavage) perfect, horizontal.
Lineation very fine and closely set, strike 180°.
Joints vertical, regular, numerous, strike 90°.

The rocks at this locality are fine-grained phyllites or slates in which grains of quartz and micaceous minerals are too small for measurement with a universal stage. Metamorphic rank, Chl_1 or Chl_2.

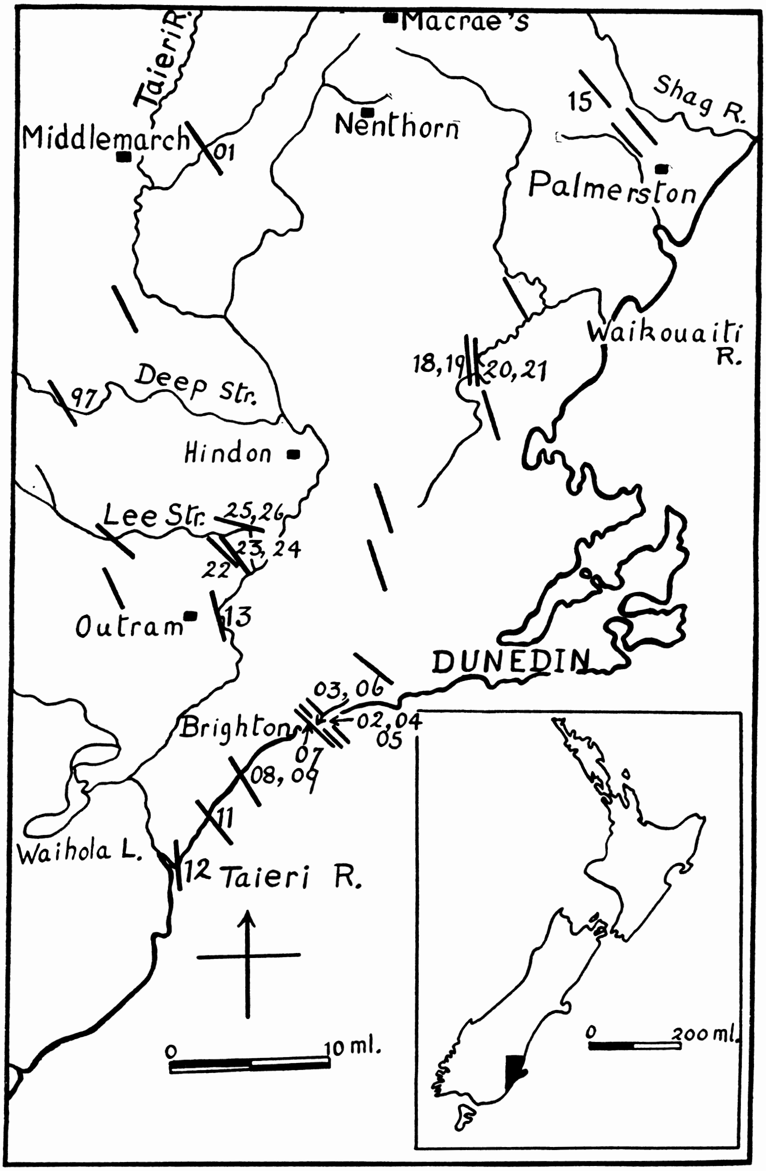

Fig. A. Map of a part of Eastern Otago. Trend of main lineation (b) in schists at representative stations is shown by solid bars. Localities of measured specimens referred to in this paper are indicated by the last two figures of the specimen number. Inset map shows the islands of New Zealand with the area here investigated in solid black.

Specimen No. 4711

Locality: East coast, three miles N of Taieri River.
Schistosity good, strike 145°, dip SW at 20°.
Lineations: *b*, strike 145°-150°; fine regular wrinkling prominent on most of the broken schistosity-surfaces;
b', strike 175°; indistinct on hand-specimen, but prominent in section parallel to *ab* where it is marked by parallel shreds of mica and stilpnomelane and by fine discontinuous banding;
b'', strike 195°; traces of irregular banding visible in section parallel to *ab*.
Joints very numerous, vertical, often filled with quartz, strike 60°-85°; also a few striking 15° and 145°.

The rock is typical of those low-rank derivatives of greywacke to which the writer has elsewhere applied the term semischist (e.g. Turner, 1935, p. 336). Schistosity is well developed but there is little trace of segregation of individual minerals into metamorphically differentiated layers. Thin sections show granular aggregates and simple clastic grains of quartz and rare, partially destroyed relicts of plagioclase, set in a fine-grained, reconstituted matrix of sericite, stilpnomelane, epidote, and undifferentiated, colourless material that is almost certainly albite and quartz. Only the coarser grains of quartz were large enough for accurate measurement with the universal stage, and fabric analysis was confined therefore to these. As seen in *ac* sections, the quartz aggregates tend to be lensoid in outline and consist of from two to ten grains with even or slightly undulose extinction. These appear to represent single clastic grains that have suffered fracture and partial recrystallization, for many of them have the optical behaviour of superindividuals, while flakes of stilpnomelane from the adjacent matrix penetrate between the component quartz grains and rarely ever cut their individual boundaries. This is borne out further by fabric analysis.

To test the degree of orientation attained in the quartz eyes, all available grains were measured in each of two sections cut at right angles to *b*, and the results were plotted as separate diagrams, Plate VI, Fig. 35 (350 grains), and Plate VI, Fig. 36 (380 grains). Comparison of the two shows that while the quartz fabric of the rock cannot be regarded as homogeneous, yet an approach to that condition has already been achieved. A

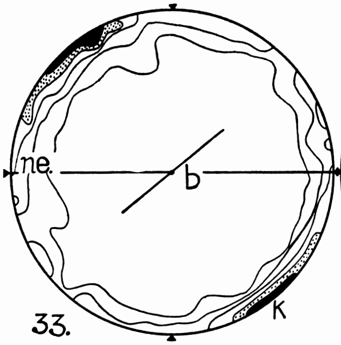

33.

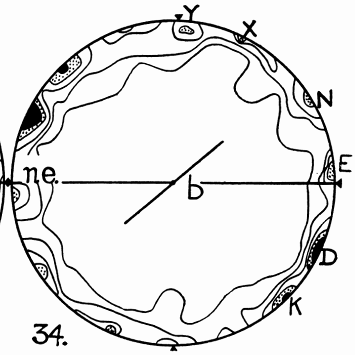

34.

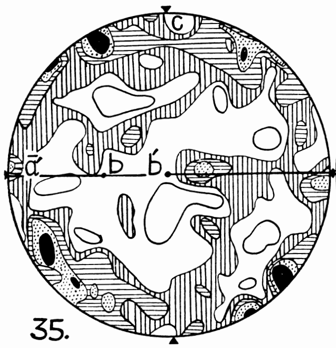

35.

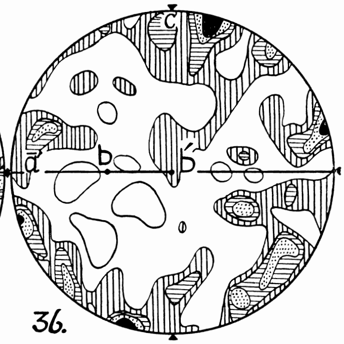

36.

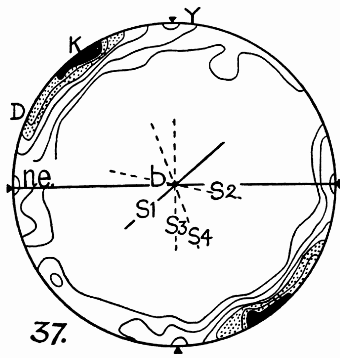

37.

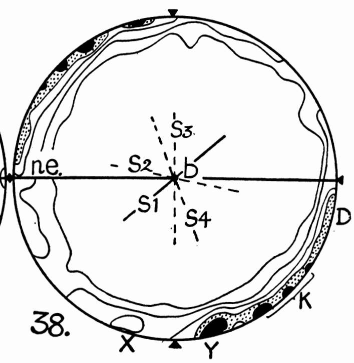

38.

PLATE VI.

Fig. 33. No. 4697, Chlorite, 200 small flakes in quartzose areas; rotated through 180° about horizontal diameter. Contours 8, 6, 4, 2, 0.5%; maximum concentration, 10%.

Fig. 34. No. 4697, Chlorite, 150 coarse flakes in chloritic aggregates; rotated through 180° about horizontal diameter. Contours 8, 6, 4, 2, 0.7%; maximum concentration, 10%.

Fig. 35. No. 4711 (Section 1), Quartz, 350 grains in lensoid aggregates; rotated through 180° about *a'*. Contours 2.5, 2, 1.5, 1, 0.3%; maximum concentration, 3.5%.

Fig. 36. No. 4711 (Section 2), Quartz, 380 grains in lensoid aggregates; rotated through 180° about *a'*. Contours 2.5, 2, 1.5, 1, 0.3%; maximum concentration, 3%.

Fig. 37. No. 4708, Muscovite, 200 flakes in thin micaceous streaks parallel to S_1; rotated through 180° about horizontal diameter. Contours 10, 8, 6, 4, 2, 0.5%; maximum concentration, 15%.

Fig. 38. No. 4708, Muscovite, 250 minute flakes in quartz-albite; rotated through 180° about horizontal diameter. Contours 8, 6, 4, 2, 0.5%; maximum concentration, 9%.

girdle has commenced to develop at right angles to b' while the areas of axial concentration, though poorly defined, nevertheless show definite similarity to those more strongly developed in diagrams for adjacent rocks (see later). There appears, from the 130 available grains measured, to be no obvious tendency toward preferred orientation of the simple clastic quartz grains, but on the other hand, the girdle pattern is strongly marked in a plot of 26 grains that make up an irregular quartzose streak resulting from incipient segregation.

The imprints of two deformations may thus be distinguished:

(1) Schistosity dipping SW at 20° is developed either by inclined movement across a tectonic axis b (145°-150°), or by subhorizontal slip across b, followed by tilting about the same axis. The lineation b owes its origin to this deformation.

(2) The features of the quartz fabric are now imprinted by slip along planes intersecting in b' (175°) and at the same time the flakes of mica and stilpnomelane are largely re-oriented parallel to the new tectonic axis, giving rise to the new lineation b'.

It is possible that these events occurred in reverse order to that given above, but the writer's interpretation is based upon assumption of analogy with rocks from the adjacent station three miles north (Nos. 4708, 4709), in which the quartz fabric was certainly imprinted after the schists in question had been folded about an axis trending at 150°.

If this interpretation is correct it follows that re-orientation of micaceous minerals during the second phase has been more effective in the fine-grained matrix of No. 4711 than in the coarser-grained laminated schists from other parts of Otago.

Specimen No. 4708

Locality: three miles S of Brighton Harbour; the schists here are thrown into open folds striking at 150° and with a crest-to-crest distance of 20 to 50 feet. No. 4708 is from the northward-dipping flank of an anticline.

Schistosity well developed, strike 150°, dip NE at 40°.

Lineation b, strike 150°, horizontal.

Joints vertical, regular, strike 60°.

The hand-specimen is from a quartzose band 15 mm. thick. The following structures are visible in the thin section cut perpendicularly to b: S_1 (megascopic schistosity) marked by continuous, narrow, undulating micaceous streaks; S_2 less prominent than S_1 but also marked by a few irregular streaks rich in mica (dip 10°-15° to SW); S_3 a vertical structure indicated by faintly developed streakiness; S_4, fractures filled with calcite, dipping SW at 70°.

The quartz diagram (Plate VII, Fig. 39) is based on measurements of 400 grains in five transverse traverses. Significant features are the girdle concentric about *b*, the maxima D and E adjacent to the pole of the horizontal plane and corresponding roughly to S_3 and S_4, the double submaximum at Y, and the absence of maxima related to the principal schistosity S_1 or to S_2.

The preferred orientation of 200 flakes of muscovite lying in micaceous streaks that mark S_1 is shown in Plate VI, Fig. 37. The single maximum K coincides with the pole of S_1 but is asymmetrically drawn out apparently under the influence of movement on the slip-planes represented by D in the quartz diagram. Plate VI, Fig. 38 was constructed from measurements of 250 smaller flakes of mica scattered through the quartz-albite areas. The maximum K is similarly drawn out toward D but there is also a strong maximum Y, apparently equivalent to Y in the quartz diagram and the girdle is complete in contrast with the incomplete girdle in Plate VI, Fig. 37; the faint submaximum at X possibly indicates the influence of S_2. The slight eccentricity of both mica girdles conforms to the condition usually observed in other diagrams for mica and chlorite and contrasts with the centred quartz girdle of Plate VII, Fig. 39.

Specimen No. 4709

Locality: as for No. 4708; collected from the southward-dipping flank of the same anticline and about ten feet distant from No. 4708.

Schistosity, well developed, strike 150°, dip SW at 30°.

Lineation *b* strike 150°, horizontal.

Joints regular, vertical, strike 60°.

In the *ac* section and corresponding surface of the hand-specimen, quartzose layers and veinlets 0.5 mm. to 3 mm. thick are separated by finely corrugated narrow micaceous bands. Within the field of the section (Fig. 43) the quartzose veinlets tend to fall into two sets, one parallel to the megascopic schistosity S_1 and the other dipping more steeply to the SW (S_2). The trend of the intervening micaceous bands while dominantly accordant with S_1 varies in different parts of the section between S_2 and the horizontal. Discontinuous steeply dipping to vertical slip-surfaces S_3 everywhere cut across the quartz veins and continue into the micaceous bands where they tend to be parallel to the axial planes of the micro-crumples; a few cracks roughly parallel to S_3 and filled with calcite were noted.

The fabric diagrams should be compared with Fig. 43, in which the structure of the rock within the measured field

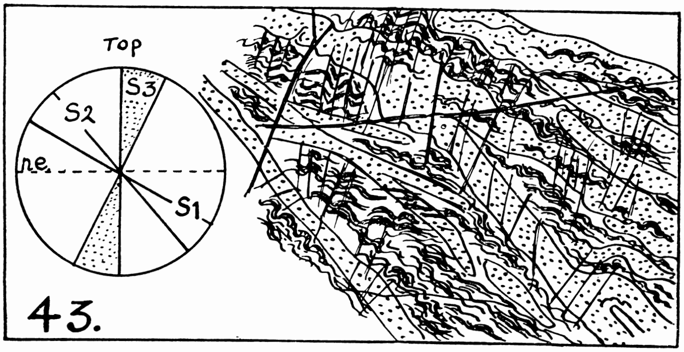

Fig. 43. No. 4709, Diagrammatic sketch of thin section cut perpendicularly to *ac*. Dotted areas = quartz veins; contorted bands = micaceous layers.

(one thin section) is represented in simplified form. The quartz diagram (Plate VII, Fig. 40) was constructed from 400 measurements. The general pattern closely resembles that of Plate VII, Fig. 39 if the trace of the horizontal plane is taken as datum for comparison. This affords clear evidence that the quartz fabric of these rocks is independent of the schistosity (S_1) and must therefore have been imprinted after the schistosity had assumed its present folded condition. The two mica diagrams, Plate VII, Figs. 41 and 42, each depict the orientation of 250 flakes, selected from the micaceous and quartzose layers respectively. Both show maxima corresponding to S_1 and S_2 together with a third concentration at Y which appears to be equivalent to similarly lettered maxima on the quartz diagrams (Plate VII, Figs. 40 and 39) and the mica maximum Y of Plate VI, Fig. 38.

The six diagrams (Plate VI, Fig. 37—Plate VII, Fig. 42) representing the fabric of specimens Nos. 4708 and 4709 are interpreted as illustrating the following sequence of events:

(1) Development of schistosity S_1, which is thrown into open folds, so that the positions of the principal mica maxima now vary according to the local orientation of S_1 in the specimens investigated.

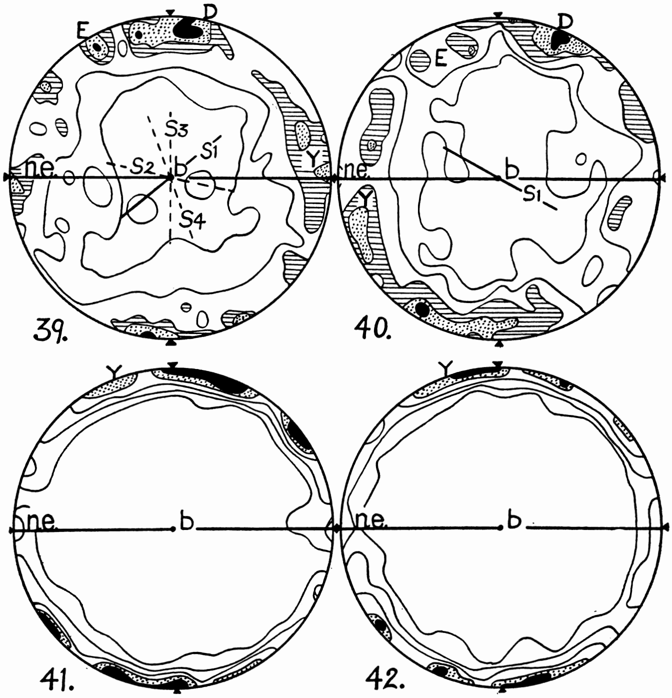

PLATE VII.

Fig. 39. No. 4708, Quartz, 400 grains; rotated through 180° about horizontal diameter. Contours 4, 3, 2, 1, 0.25%; maximum concentration, 4.5%.

Fig. 40. No. 4709, Quartz, 400 grains; rotated through 180° about horizontal diameter. Contours 4, 3, 2, 1, 0.25%; maximum concentration, 4.5%.

Fig. 41. No. 4709, Muscovite, 250 flakes in micaceous bands; rotated through 180° about horizontal diameter. Contours 8, 6, 4, 2, 0.4%; maximum concentration, 10%.

Fig. 42. No. 4709, Muscovite, 250 flakes in quartzose layers; rotated through 180° about horizontal diameter. Contours 8, 6, 4, 2, 0.4%; maximum concentration, 9%.

(2) Movement on gently inclined slip-surfaces giving rise to the submaxima Y in both mica and quartz diagrams. In each rock this is more strongly developed for the mica-in-quartz than for the mica-in-mica fabric. S_2 also probably belongs to this stage of deformation.

(3) Movement on steeply inclined slip-surfaces, imprinting the main features of the quartz fabric (maxima D and E) but leaving the mica almost unaffected.

Specimen No. 4707

Locality: Trigonometrical survey-station DD, north point of Brighton Harbour.

Schistosities: S_1 horizontal, obvious in the outcrop but poorly developed in hand-specimen; S_2, strike 130° (ranging in various nearby localities from 130° to 140°), dip SW at 30° to 40°.

Lineations: *b* (intersection of S_1 and S_2) prominent, strike 130°; *b′*, occasionally visible on S_2, strike 150° to 160°.

Joints vertical, strike 50° to 60°.

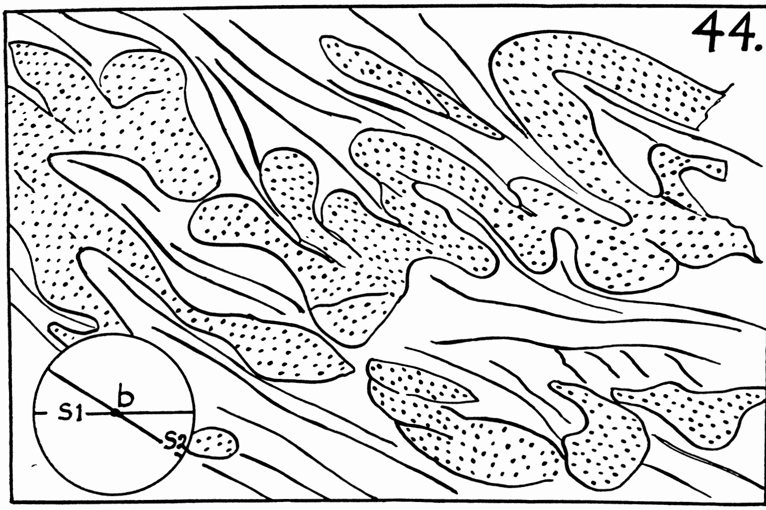

Fig. 44. No. 4707, Diagrammatic sketch of measured part of thin section cut perpendicularly to *ac*. Dotted areas are quartzose layers.

Surfaces cut normal to *b* show intense contortion and small-scale recumbent folding of white quartzose layers 1 mm. to 2 mm. in thickness, with S_2 as axial plane (cf. Fig. 44). The detail of a small part of one of these crumpled layers as seen in the measured thin section is indicated diagrammatically in Fig. 44. The quartz diagram, Plate VIII, Fig. 45, based on measurements of 350 grains, conforms to the general pattern of previous figures, except that in the present diagram the maxima are rather more widely spread than usual. Whereas maxima E and N might well be related to slip movements involved in or subsequently moulded on the crumpling process,

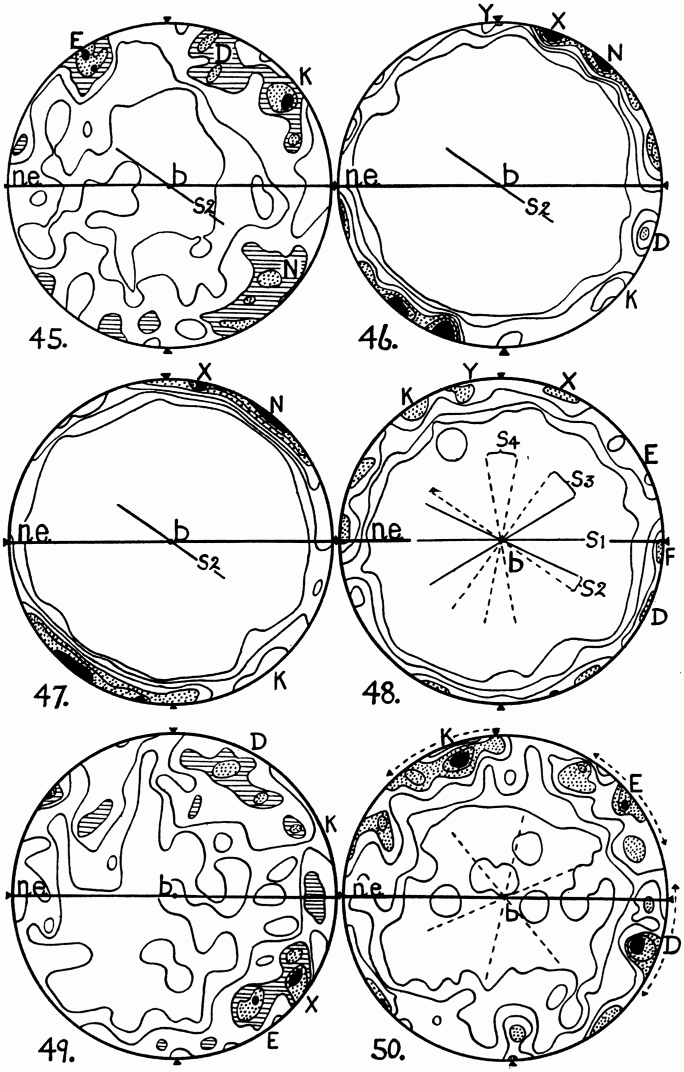

PLATE VIII.

Fig. 45. No. 4707, Quartz, 350 grains. Contours 4, 3, 2, 1, 0.3%.

Fig. 46. No. 4707, Muscovite, 150 flakes in quartzose areas. Contours 10, 8, 6, 4, 2, 0.7%; maximum concentration, 12%.

Fig. 47. No. 4707, Muscovite, 300 flakes in micaceous layers. Contours 10, 8, 6, 4, 2, 0.3%; maximum concentration, 12%.

Fig. 48. No. 4702, Muscovite, 200 flakes. Contours 6, 4, 2, 0.5%; maximum concentration, 7%. *s*-planes visible in measured specimen indicated by full lines; *s*-planes visible only in Nos. 4704, 4705 (adjacent specimens) indicated by broken lines.

D and K have no obvious relation of this sort and presumably are the result of late slip cutting across the folded structure.

Mica diagrams were prepared for 150 small, clear-cut flakes enclosed in the quartzose layers (Plate VIII, Fig. 46) and for 300 sharply crystallized flakes in the micaceous bands (Plate VIII, Fig. 47). The two figures are similar in that each possesses a girdle centred about *b* with strong maxima at N (= S_2) and X. Submaxima K and D correspond well with concentrations similarly lettered in the quartz diagram.

Specimens Nos. 4702, 4704, 4705

Locality: South end of Green Island Beach, one-half mile north of Brighton Harbour; all three specimens collected from within a radius of 5 yds.

Lineation *b* very prominent, horizontal, strike 130°; parallel to intersection of sets of *s*-planes S_1 etc.

Joints vertical, strike 50°-60°; a few very prominent joints strike at 130°.

Schistosities poorly differentiated: S_1 (horizontal) faintly developed, but emphasized by parallel quartz veins 2 mm. to 3 mm. thick; S_2 (dip SW at 25° to 30°) shows up as a direction of streaking in thin sections cut parallel to *ac* from all three specimens; S_3 (dip NE at 30°-50°) is the most prominent set of *s*-planes in both sections and hand-specimens; S_4 (nearly vertical) is faintly visible in *ac* sections cut from Nos. 4704 and 4705.

In the mica diagram (Plate VIII, Fig. 48) showing orientation of 200 flakes of muscovite in specimen No. 4702, the *b*-girdle is more nearly complete and the maxima less prominent than usual, as indeed might be expected from the number and poorly differentiated condition of the visible *s*-surfaces. S_2, S_3, and S_4 appear to be represented by maxima at X, K, and D, respectively, but the influence of S_1 is hardly discernible. The diagram (Plate VIII, Fig. 49) for 250 grains of quartz in the same rock also shows several maxima, the strongest of which (X) occupies a position corresponding with S_2 and is thus equivalent to X of the mica diagram. D and K are also correlated with similarly lettered points in Plate VIII, Fig. 48,

---

Fig. 49. No. 4702, Quartz, 250 grains. Contours 4, 3, 2, 1, 0.4%.

Fig. 50. No. 4702, Calcite, 200 grains. Contours 5, 4, 3, 2, 1, 0.5%. Dotted lines at centre indicate directions of deduced slip-surfaces corresponding to the three ring maxima at D, E, and K. Dotted arcs subtend angles of 40°.

while a strong concentration of quartz axes at E seems to be equivalent to a faintly indicated submaximum in the diagram for mica. The separate identities of E and X in Plate VIII, Fig. 49 are brought out by the development of X in the mica diagram and of E in the diagram for calcite. The latter (Plate VIII, Fig. 50) shows the orientation of the optic axis in 200 grains of calcite from the same section as that in which quartz and mica were measured. The grains are invariably untwinned but sometimes show traces of a lamellar structure parallel to the flat rhombohedron *e*, presumably the result of translation-gliding. The calcite diagram clearly shows a girdle approximately centred at *b*. Interpretation of the maxima is less certain than in the case of the quartz diagram, since it was found impossible to test the homogeneity of the calcite fabric on account of the small number of grains available. Assuming homogeneity, it would seem reasonable from analogy with calcite diagrams published by other writers (e.g. Sander, 1930, D 73, 81, 82, etc.) to interpret the maxima grouped at D, E, and K in Plate VIII, Fig. 50 as ring maxima developed by rhombohedral gliding on three sets of *s*-surfaces (broken lines in Plate VIII, Fig. 50). These *s*-surfaces so deduced would coincide with those indicated in the quartz diagram by D (S_4), E, and K (S_3). The relative positions of correlated maxima for mica, quartz and calcite are given in the following table in terms of angular distance measured clockwise around the circumference from the horizontal diameter of the diagram (quartz, visible *s*-planes) or from the vertical diameter (mica, calcite) as the case may be.

Maximum and Corresponding s-plane	Angular Distance Clockwise from Polar Diameter of Diagram		Angular Distance Clockwise from Equatorial Diameter of Diagram	
	Mica	Calcite	Quartz	Visible S in No. 4702
X (S_2)	25°		30°	25°
E	50-65°	50°	55°	
F (S_4*)	95°			
D	115°	105°	110°	
K (S_2)	150°	155°	150°	150°
Y (S_1)	165°			0°

In the diagram for quartz (Plate VIII, Fig. 49), the concentrations D-K and E-X might possibly be interpreted as two

* S_4 is visible only in Nos. 4704 and 4705.

ring maxima developed by rhombohedral gliding. On this hypothesis the orientation would be controlled by slip on *s*-planes situated respectively at angular distances of 35°-40° (D-K) and 130°-135° (E-X) measured clockwise from the equator. These values do not agree with the recorded positions of mica and calcite maxima, and of visible *s*-surfaces as set out in the above table. On the other hand there is close agreement if the quartz maxima D, K, X, E are interpreted as the expression of a tendency for alinement of the quartz axes parallel to four sets of slip-surfaces in the rock fabric.

In the above discussion, assumption of homogeneity of the quartz fabric seems justified by analogy with the substantial homogeneity established for the quartz fabrics of neighbouring rocks that have been investigated in greater detail. The assumed homogeneity of the calcite fabric on the other hand is by no means proved.

Specimens Nos. 4703, 4706

Locality: 200 yds. S of locality for No. 4702, etc.

Lineation *b* very prominent, horizontal, strike 135°-140°; produced by intersection of several sets of schistosity surfaces.

Joints vertical, strike 50°-60°; a few at 135°.

Schistosities rather more distinct than in No. 4702, etc.; S_1 (dip NE at 0°-10°) faintly indicated in hand-specimen; S_2 (dip SW at 25°-45°) is the most prominent direction of banding and one of the directions of easy cleavage; S_3 (dip NE at 60°-70°) is a second direction of ready cleavage, indicated in thin section by micaceous streaks and vaguely defined bands of finely crystalline quartz cutting the massive quartz layers; S_4 vertical, indicated only in No. 4706 by faint cleavage and slight tendency for development of parallel strings of mica in the thin section.

The structure is complicated by the presence of quartzose segregation-bands 5 mm. to 8 mm. thick, which, though much contorted and ruptured, trend parallel to S_2 within the limits of the measured section of No. 4703.

Plate IX, Figs. 51 and 52, are diagrams for muscovite (300 flakes) and quartz (400 grains) respectively. The former is relatively simple, with a single strong maximum N corresponding to S_2 but elongated eccentrically in a clockwise direction as the result of a tendency, obvious in thin section, for the mica flakes to lie somewhat obliquely to S_2; there are also faint

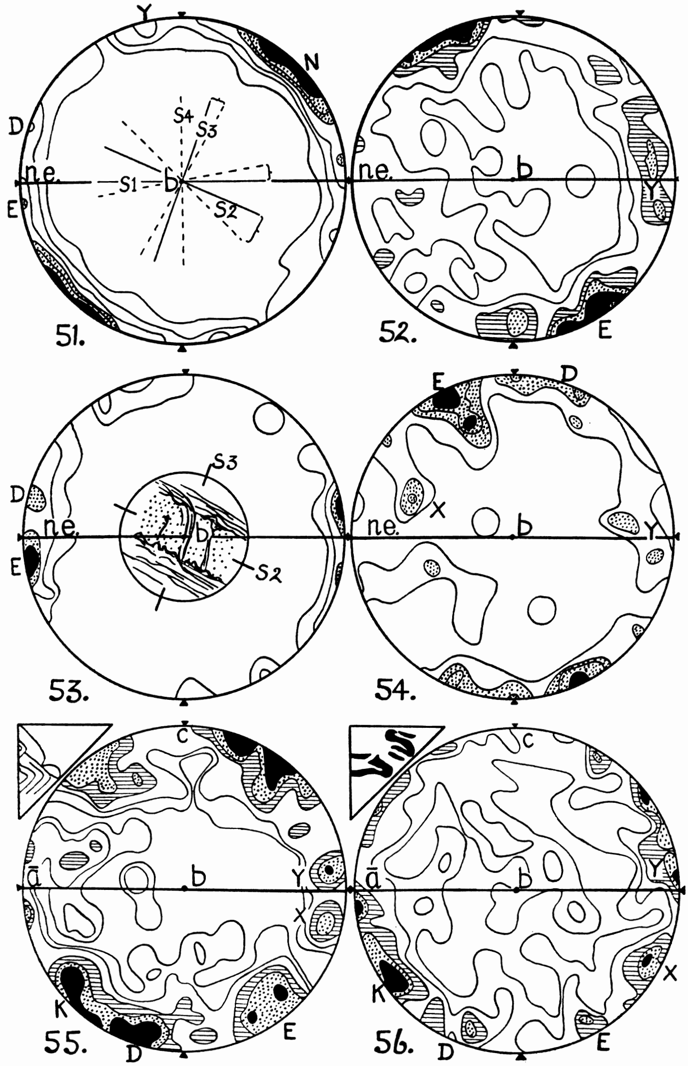

Plate IX.

Fig. 51. No. 4703, Muscovite, 300 flakes; rotated through 180° about horizontal diameter. Contours 10, 8, 6, 4, 2, 0.3%. Full lines at centre indicate *s*-surfaces for No. 4703; broken lines *s*-surfaces for No. 4706.

Fig. 52. No. 4703, Quartz, 400 grains; rotated through 180° about horizontal diameter. Contours 4, 3, 2, 1, 1.25%; maximum concentration, 5%.

Fig. 53. No. 4703, Muscovite, 50 flakes in bands parallel to S_3 cutting quartzose layer; rotated 180° about horizontal diameter. Contours 14, 10, 6, 2%.

Fig. 54. No. 4703, Quartz, 80 grains in fine-grained band parallel to S_3 cutting coarser quartzose layer; rotated 180° about horizontal diameter. Contours, 7, 5, 3, 1%.

submaxima Y and D reflecting the influence of S_1 and S_3, and a third, somewhat stronger one, E, the significance of which will be discussed below. The quartz diagram, Plate IX, Fig. 52, conforms well to the usual Otago type except that the concentration of steeply alined quartz axes is asymmetric with reference to the pole of the horizontal plane. The divided submaximum at Y, so commonly seen in other diagrams for quartz in Otago rocks, is present in Plate IX, Fig. 52 also.

Additional diagrams, the data of which are not included in Plate IX, Figs. 51 and 52, have been prepared respectively for muscovite (Plate IX, Fig. 53; 50 flakes) and quartz (Plate IX, Fig. 54; 80 grains) lying in a narrow zone trending parallel to S_3 and cutting sharply across the main quartzose band. The micas here build up discontinuous streaks defining S_3, but near the boundaries of the quartz-rich band in which they are enclosed they commence to curve and then pass without apparent break into streaks in the adjacent matrix where the trend is now parallel to S_2 (cf. inset circle of Plate IX, Fig. 53). A pronounced maximum at D in Plate IX, Fig. 53 corresponds with the mean direction of S_3, but there is an even stronger concentration some 30° distant at E, a condition depending rather upon the curved course of S_3 than upon the existence of a second set of *s*-surfaces. The latter possibility must not be excluded entirely, however, since E in Plate IX, Fig. 53 is in approximately equivalent position to the principal maximum of the quartz diagrams. It may here be noted that the maxima D and E in Plate IX, Fig. 53 are reproduced by faint submaxima in Plate IX, Fig. 51.

The quartz grains that constitute the basis of Plate IX, Fig. 54 are smaller than those of the enclosing quartzose "vein" and show a decided tendency toward dimensional elongation parallel to S_3. The diagram, however, is closely similar to the main quartz diagram (Plate IX, Fig. 52), especially as regards the strength and position of maxima E and Y. A submaximum at D (absent in Plate IX, Fig. 52) seems significant, for it suggests a tendency for alinement of some quartz

---

Fig. 55. No. 4715, Quartz, 213 grains in area A of Fig. 57. Contours 4, 3, 2, 1, 0.5%; maximum concentration, 6%. Structure of measured area is shown in top left corner.

Fig. 56. No. 4715, Quartz, 250 grains in folded quartzose layers adjacent to B and C, Fig. 57. Contours 4, 3, 2, 1, 0.4%; maximum concentration, 5%. Outline of measured area is shown in black in top left corner.

axes in S_3. Similarly, X in Plate IX, Fig. 54 may indicate a tendency for the quartz axes to lie in S_2, but in view of the small number of measured grains and the absence of any corresponding submaximum in Plate IX, Fig. 52, its presence should probably be regarded as fortuitous.

The following sequence of events is put forward to account for the fabric data recorded above:

(1) Development of S_3.

(2) Initiation of transverse slip-surfaces parallel to S_2, with parallel growth of segregation "veins" rich in quartz locally enclosing the original S_3 structure [A corresponding stage of development is illustrated by schists from Waipori described in a previous paper (Turner, 1938, a, Figs. 1, 12)].

(3) With continued differential movement in the micaceous layers, S_3 becomes transposed into its present position S_2 and the original trend is preserved only where S_3 was enclosed within the massive quartz "veins"; the latter also become contorted and ruptured within the field of the hand-specimen. Note that the flakes of mica in the micaceous matrix now tend to lie with (001) inclined slightly to the new S_2 as a result of lag in the transposition process; hence the clockwise elongation of maximum N in Plate IX, Fig. 51.

(4) Movement on a steeply inclined set of *s*-surfaces dipping SW almost obliterates the early quartz fabric and alines the quartz axes in the new direction (maximum E) without appreciably affecting the mica fabric.

At what stage slip-surfaces parallel to S_1 came into existence is not clear, but the weakness of the corresponding mica and quartz maxima (Y) suggests that movement on these surfaces was relatively unimportant.

It is reasonable to assume that in the nearby rocks represented by No. 4702 (Plate VIII, Fig. 48—Plate IX, Fig. 51) a similar sequence of events should hold good. In these rocks, however, movement at the third stage was apparently not sufficiently intense to cause complete transposition of the original *s*-surfaces (S_3). S_3 therefore remains the most prominent direction of banding, with S_2 as a subsidiary set of *s*-surfaces crossing the first. Also, the final imprint of the quartz fabric involved movement on steep slip-surfaces dipping both SW and NE instead of only SW as in No. 4703, and this affected calcite and mica as well as quartz.

Tilted Schists From District Centering Around Palmerston.

In the north-eastern part of the map in the general vicinity of Palmerston the schists of the Maniototo Series have been mapped by H. Service (1933) and O. D. Paterson,[10] who find that an inclined condition with SE dips of 15° to 30° about a more or less NE axis is general, though local variations of both strike and dip are also recorded, especially in the vicinity of late Tertiary faults. Mr. Paterson has noted widespread small-scale contortion of the schistosity-surfaces over much of the area mapped by him and has kindly supplied the writer with specimens for fabric analysis, one of which (No. 4715) is described below in detail.

Specimen No. 4715

Locality: one and one-half miles SW of trigonometrical survey station S, Moeraki Survey-district.

Schistosity well developed, strike 30°, dip SE at 30°.

Lineation *b* prominent, strike 145°-150°, pitch SE at 25°. (This general NW-NNW trend of the lineation is almost constant in the district mapped by Paterson and appears to be independent of the strike of the schistosity).

Trend of joints not recorded.

The highly complex structure of the hand-specimen as illustrated by sketches in Fig. 57 is interpreted by the writer as the result of metamorphism in three phases:

(1) Alternating micaceous and quartzo-feldspathic layers develop by segregation of the various constituents during reconstitution of the rock—a process of metamorphic differentiation during deformation.

(2) The resultant highly inhomogeneous rock is further deformed by a process of flexural-slip folding, which culminates in rupture of the resistant quartzose layers into bodies of irregular outline around which has been drawn the laminated micaceous matrix with its parallel structure produced by ultimate shearing-out of fold crests in the contorted mica-rich layers. This explanation for the origin of such structural details as are figured in the lower half of Fig. 57 agrees with the conceptions of Heim and of Sander as to the evolution of transposition cleavages (*Ausweichungsclivage* and *Umfaltungs-*

[10] Geology of the Lower Shag Valley, ms. in course of preparation for publication in *Transactions of Royal Society of N. Z.*

clivage) by extreme small-scale folding (cf. Sander, 1930, p. 252, Fig. 122; Knopf, 1931, pp. 14-19, Figs. 7-10).

(3) Post-deformational crystallization of most of the constituent minerals must be assumed, to account for the sharp, undistorted outlines of most of the flakes of muscovite and chlorite, even where these are alined along the sinuous slip-surfaces that everywhere traverse the section, and to explain the absence of obvious granulation in the quartzose layers;

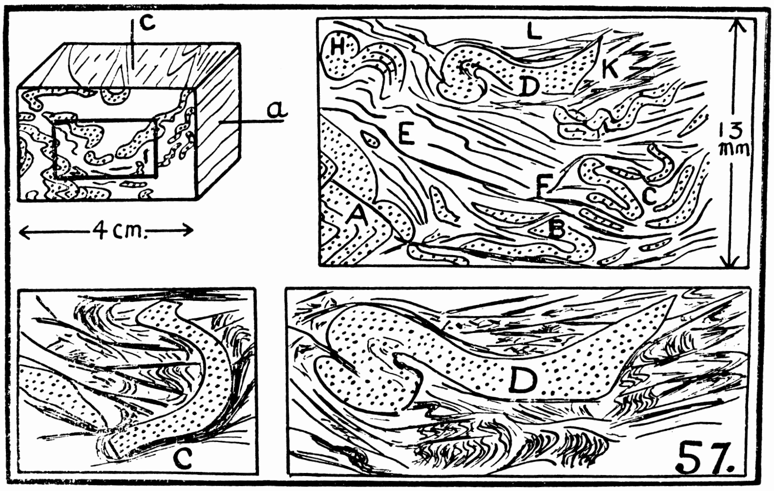

Fig. 57. No. 4715, Sketches of structures visible in hand-specimen (top left) and corresponding thin section cut at right angles to *b* (top right). Details of parts of same section are shown in the two lower sketches. Quartzose areas stippled. Approximate position of section is indicated by small rectangle in the top left figure; lack of correspondence in structural details is due to the hand-specimen having been cut for polishing about 1 cm. back from the position occupied by the section slice.

further there are several patches of clear quartz, chlorite, and mica without obvious preferred orientation, that occupy spaces enclosed in the crests of folded resistant bands or adjacent to ruptured fragments of these latter.

This rock, like the majority of the schists of eastern Otago so far investigated, is thus a blasto-phyllonite—a rock in which growth of crystals has outlasted the phyllonitization of the original greywacke. It remains to determine further from fabric diagrams to what extent the fabric has been affected by movements not related to the visible slip-surfaces, to what extent any pre-deformational fabric may have been preserved

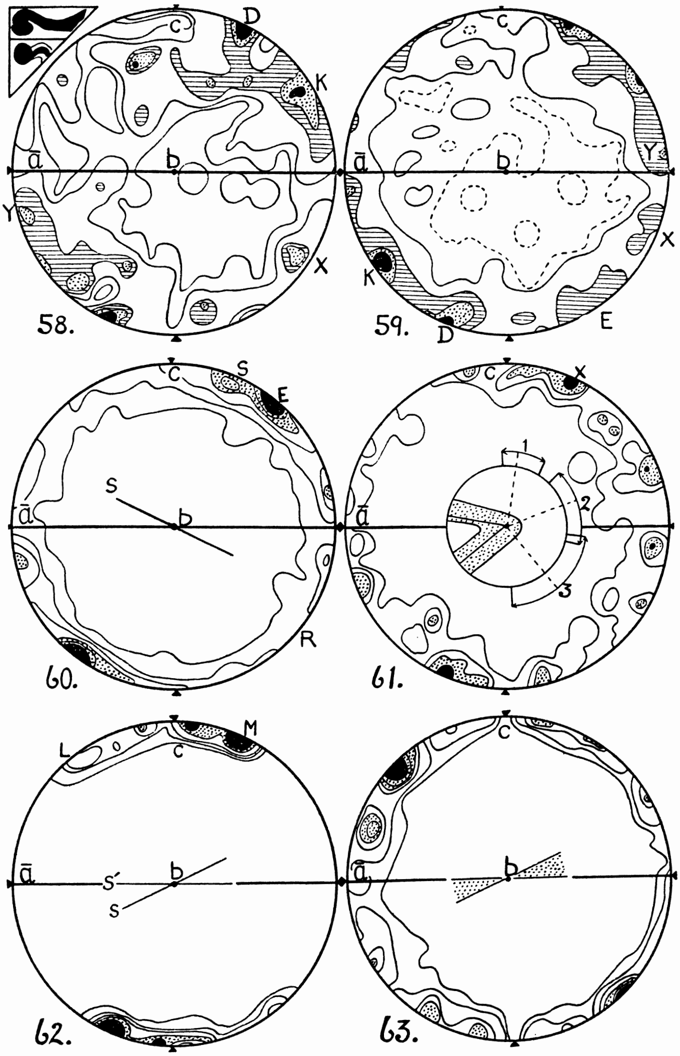

PLATE X.

Fig. 58. No. 4715, Quartz, 170 grains in folded quartz layers D and H, Fig. 57. Contours 4, 3, 2, 1, 0.5%; maximum concentration 4.5%. Outline of measured areas is shown in black in top left corner.

Fig. 59. No. 4715, Quartz, collective diagram of 633 grains included in Figs. 55, 56, 58. Contours 4, 3, 2, 1, 0.5%; maximum concentration, 4%.

Fig. 60. No. 4715, Muscovite, 300 flakes in visible slip surfaces in micaceous matrix between E and F of Fig. 57. Contours 10, 8, 6, 4, 2, 0.3%; maximum concentration, 14%. S = mean trend of dominant visible slip-surfaces within area measured.

Fig. 61. No. 4715, Muscovite, 73 flakes enclosed in quartz-albite area A of Fig. 57. Contours 8, 6, 4, 2, 1%; maximum concentration, 8%. Inset figure shows orientation of fold within which micas were measured; broken lines are normals to the limbs and crest respectively.

Fig. 62. No. 4715, Muscovite, 56 flakes lying in visible slip-surfaces of area K in Fig. 57. Contours 20, 16, 12, 8, 2%. S and S′ = trends of observed slip-surfaces.

Fig. 63. No. 4715, Muscovite, 130 flakes lying between visible slip-surfaces of areas L and K in Fig. 57. Contours 10, 8, 6, 4, 2, 0.8%. Dotted sector at centre shows range of visible slip-surfaces within the areas measured.

in the quartz-rich layers (cf. Sander, 1930, p. 257), and whether the quartz fabric is homogeneous or otherwise. With this purpose, partial and collective diagrams for quartz and muscovite were prepared, some of which are reproduced as Plate IX, Figs. 55, 56, Plate X, Fig. 58—Plate XI, Fig. 65.

Plate IX, Fig. 55 represents 213 grains of quartz measured within the folded area A of Fig. 57; Plate IX, Fig. 56 is based on 250 quartzes in the ruptured layers B-C, while the orientation of 170 grains in areas D and H is shown in Plate X, Fig. 58. For each area, several partial diagrams representing orientation within restricted parts of the area in question were first prepared separately,[11] and were later combined only after it was found that the general patterns of the component diagrams were essentially similar. For each of the three measured areas the quartz fabric would thus appear to be relatively homogeneous in spite of the complexity of local structure. However, the small number of grains available in the component sectors (usually 50 to 70) renders a certain degree of divergence unavoidable even if the fabric is fairly homogeneous, and conversely would make it difficult to detect a relict fabric capable of being "unrolled" (cf. Sander, 1930, p. 257) if this were poorly defined.

Further evidence of an approach to homogeneity is afforded by the mutual similarity of Plate IX, Figs. 55, 56, and Plate X, Fig. 58, and the resemblance of each to the collective diagram, Plate X, Fig. 59. The features persistently present are a well defined girdle centred approximately at *b*, maxima or submaxima at points lettered K, D, E, X, Y, and a tendency for maxima to be stronger in the top right and bottom left than in the other two quadrants. On the other hand, it is also clear from the diagrams that a perfectly homogeneous quartz fabric has not been attained, for there is some variation both in strength and exact position of the maxima. It will be noted how, in such a case as this, where some degree of inhomogeneity of fabric persists, the diagram becomes simplified and the peripheral position of the maxima emphasized when a sufficiently large number of grains are measured (633 for Plate X, Fig. 59).

The preferred orientation of the quartz as pictured in any

[11] For example, partial diagrams were plotted separately for the two limbs and the crest of the fold A, for area D and area H, and for limbs and crests of folds B and C.

one of Plate IX, Figs. 55, 56, Plate X, Figs. 58, or 59 may be interpreted as the result of either one of two alternative processes: external rotation of the whole fabric by flexural slip about b (= B) giving a non-homogeneous resultant fabric, or slip along more than one set of slip-surfaces intersecting in b (= B) giving a homogeneous fabric as end-product. Flexural slip is certainly largely responsible for the complex configuration of the quartzose layers. But the substantial homogeneity of the quartz fabric both within a single folded sector (such as A of Fig. 57) and within the limits of the measured thin section (cf. Plate X, Fig. 59) strongly favours the conclusion that late movements on several sets of intersecting slip-surfaces have been the main factors that determined the present preferred orientation of the quartz. According to the writer's interpretation, the mean trends of these slip-surfaces are indicated in Plate X, Fig. 59 by maxima K, D, E, X, and Y. Local deviation from the mean trend is to be expected in a mechanically inhomogeneous rock of this type and would account for the minor inhomogeneity of the quartz fabric and corresponding slight discrepancies between the partial diagrams. Thus, in the partial diagrams prepared for the folded area B of Fig. 57, it was found that maximum X is more strongly developed in the diagram based on grains in the crest than in those representing grains in the limbs of the fold, indicating that slip in the crest tended to be localized in planes parallel to the axial plane of the fold.

Finally it is to be noted that maxima X and Y could be developed by movements along surfaces parallel to the visible slip-planes in the micaceous matrix (i.e., subparallel to the schistosity), and they are so interpreted here. The stronger maxima, K, D, and E, on the other hand, are unrelated to visible slip-planes but, as will be shown below, correspond well with maxima in some of the mica and stilpnomelane diagrams.

For purely descriptive purposes, four types of muscovite may be distinguished:

(a) Relatively coarse flakes building up films of mica often clouded with finely divided opaque iron-ore (?), which have been spread out along the visible slip-surfaces.

(b) Somewhat smaller flakes making up short, sinuous transverse streaks between the visible slip-surfaces. These probably in part represent crests of microfolds that have been sheared out during deformation (cf. lower sketches of Fig. 57).

(c) Flakes without visible orientation occurring as constituents of quartz-mica-chlorite eyes bounded by the visible slip-surfaces.

(d) Rather coarse, isolated, apparently unoriented crystals, which together with stilpnomelane, quartz, and chlorite build up rare, rather large patches that seem to have crystallized after cessation of the main deformation, often in areas protected by the more rigid quartzose portions of the section.

(e) Minute flakes sparsely scattered in the quartzose layers. Crystals of types (c), (d) and (e) are always undeformed, clear-cut flakes; the same is true for most of the mica classed under (a) and (b) but occasionally these latter have been slightly bent.

The diagrams for mica in a rock of such complicated structure need careful interpretation, for several maxima may represent a single contorted set of *s*-surfaces in a non-selective diagram. On the other hand, preparation of selective diagrams should bring out the presence of hidden *s*-surfaces if these are present.

Plate X, Fig. 60 is a typical non-selective diagram based on total mica (300 flakes) encountered in several traverses across the schistosity in the mica-rich areas marked E and F in Fig. 57. The trend of the principal visible *s* is fairly constant in the two areas and in both cases mica of type (a) predominates, though types (c) and to a less extent (b) are also represented. The two partial diagrams, for E and F respectively, agree perfectly so that only the collective diagram, Plate X, Fig. 60, is reproduced here. This is relatively simple, with a girdle centred at *b* and a strong maximum E corresponding approximately with the pole of the mean visible *s*-surfaces. The distinct eccentricity of this maximum and of the complementary minimum R in relation to *s* is repeated in both partial diagrams and cannot therefore be fortuitous. It could be due either to oblique alinement of the micas lying in *s*, to oscillatory movement in *s* or to the influence of mica in the intervening eyes. This latter is no doubt expressed also in the submaxima on either side of the pole of the *a* reference axis.

Plate X, Fig. 61 is also a non-selective diagram representing the orientation of 73 flakes of mica enclosed within the folded quartz-albite layer A of Fig. 57, and serves to illustrate once more the girdle pattern that dominates orientation of the mica. From the distribution of the maxima through a wide arc it is clear that there is no single dominating set of parallel *s*-surfaces such as would be expected in a pure slip-fold, so that origin of the fold by flexural slip is probable. This conclusion is clinched when the partial diagrams on which Plate X, Fig. 61 is based are considered. Of the flakes lying in the upper limb 50 per cent are oriented within the arc numbered 1 in the inset figure, while 85 per cent of the micas from the fold crest lie within arc 2.[12] On the other hand the flakes of the lower limb instead of being concentrated within arc 3 are almost evenly distributed through the girdle; actually only 45 per cent lie within arc 3 which is equivalent to about 40 per cent of the complete girdle. The probable explanation is that flexure-folding was followed by uniform slip in planes slightly oblique to the upper but almost transverse to the lower limb (cf. Fig. 64b). The principal maximum X, including many poles of flakes in the lower limb, gives the approximate trend of this late slip, and indeed a well defined fracture correspondingly oriented actually cuts across the fold-system in question and is lined with parallel undeformed mica crystals (not included in Plate X, Fig. 61).

Plate X, Fig. 62 is one of several selective diagrams illustrating orientation of mica of type (a), i.e. the coarse flakes, lying within the films that mark the visible surfaces of slip, and is based upon measurements of 56 flakes in area K of Fig. 57, where two sets of slip-surfaces S and S′ are clearly shown. The influence of flakes alined in S is expressed in submaximum L, but the sharp discrepancy between maximum M representing poles located in S′ and the pole of S′ itself shows a strong tendency for these crystals to lie obliquely to the *s*-planes in which they are situated (cf. Fig. 64c). Various explanations are possible. The oblique micas might represent a relict *s*-structure preserved in S′ or a later structure superposed upon S′, though this latter alternative is rendered improbable by the conformable orientation of crystals located in S. On the other hand, the condition observed in S′ could be accounted for by clockwise rotation of micas originally alined in S′ as a result of differential movement in a new set of planes S involving uniform left-to-right displacement of the upper with reference to the lower layers (cf. Plate XI, Fig. 65c). Such

[12] The percentage quoted includes poles on the two diametrically opposite sectors of the girdle.

minute-scale left-to-right (NE to SW) "overthrusting" is in any case indicated by the present outlines of the folded and ruptured quartz layers throughout the specimen as a whole (cf. Fig. 57).

Plate X, Fig. 63 is constructed from a plot of 130 poles of micas of types (b) and (c) between the slip-surfaces of areas K and L (Fig. 57). The girdle pattern is well brought out,

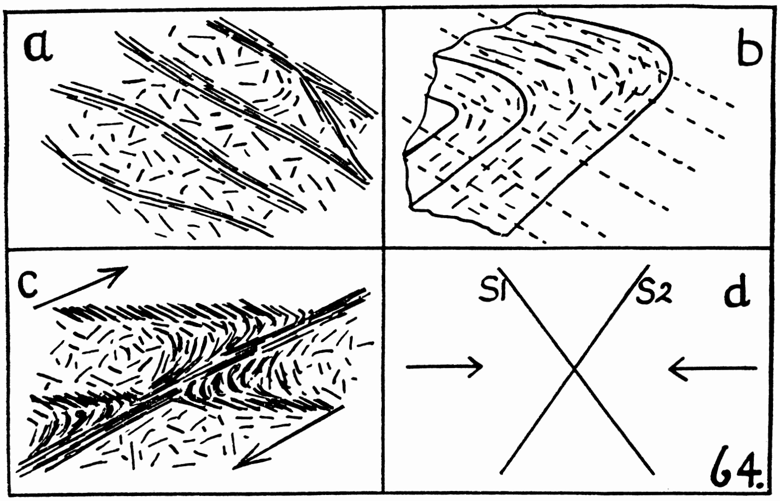

Fig. 64. No. 4715, Idealised sketches illustrating the orientation of mica in different parts of the section perpendicular to *b* as deduced from the fabric diagrams: (a) mica in subparallel slip-surfaces and intervening eyes (Fig. 60); (b) mica in folded quartzose layer affected by late slip parallel to broken lines (Fig. 61); (c) mica obliquely alined in horizontal slip-surfaces cut by inclined surfaces in which the micas are parallel (Fig. 62); arrows indicate probable direction of movement on the inclined surfaces; (d) principal slip-surfaces and direction of causal compression responsible for orientation of late mica and stilpnomelane (Figs. 65, 66).

but further interpretation of the diagram would be unsafe since the exact positions of the maxima, based as they are upon two types of transverse and oblique micas, are probably fortuitous.

The orientation of mica and stilpnomelane probably of late origin, from the apparently undeformed aggregates mentioned under type (d) above is illustrated by Plate XI, Figs. 65 and 66 respectively, each based upon 100 measurements. The diagrams are strikingly similar as regards both maxima and submaxima, and it is therefore safe to draw conclusions from the data so represented. The principal maxima D and E of Plate XI, Fig. 65 and their complementary minima at appropriate points in the girdle are reproduced in the stilpnomelane diagram (Plate XI, Fig. 66) and suggest the influence of hidden *s*-planes S_1 and S_2 as shown in Fig. 64d. These coincide almost exactly with the *s*-surfaces deduced to account for maxima D and E in the quartz diagram, Plate X, Fig. 59. There is also exact correspondence between maximum Y of Plate XI, Fig. 65 (less prominent but accurately situated in Plate XI, Fig. 66) and the similarly lettered point on the quartz diagrams.

On the evidence of the fabric data discussed above, the metamorphic history of the rock as set out earlier in this section is now elaborated as follows:

(a) After contortion and rupture of the quartzose layers in the main stage of deformation, a more or less uniform penetrative movement of slip seems to have affected quartzose and micaceous layers alike on a gently inclined set of *s*-surfaces expressed by maxima X in the quartz diagrams and in Plate X, Fig. 61, and possibly maximum M in the mica diagram, Plate X, Fig. 62. Maxima Y in Plate X, Fig. 59, Plate XI, Figs. 65, 66, probably also date from this stage which is regarded as the final phase of the main deformation.

(b) The latest recorded movements were initiated on two sets of steeply inclined intersecting *s*-surfaces, of which maxima D and E in the diagrams for quartz, late mica, and stilpnomelane (Plate X, Fig. 59, Plate XI, Figs. 65, 66) are the visible expression. Plate XI, Fig. 65 in particular shows almost ideal orthorhombic symmetry, and typifies the theoretically expectable diagram for mica affected by simultaneous slip on two equally developed sets of *s*-planes during a simple horizontal compression (cf. Fig. 64d). A corresponding orthorhombic symmetry is closely approached in Plate IX, Fig. 55, which depicts the preferred orientation of quartz in the most rigid mass of quartzose material in the measured section.

(c) Maximum K of the quartz diagrams is without counterpart in the diagrams for muscovite and stilpnomelane and its interpretation is therefore uncertain. Possibly K and D together constitute a split maximum resulting from slight oscillation (about *b*) in a single set of slip-planes.

(d) Throughout the whole history of deformation so far deduced the tectonic axis *b* (= B) has remained approximately

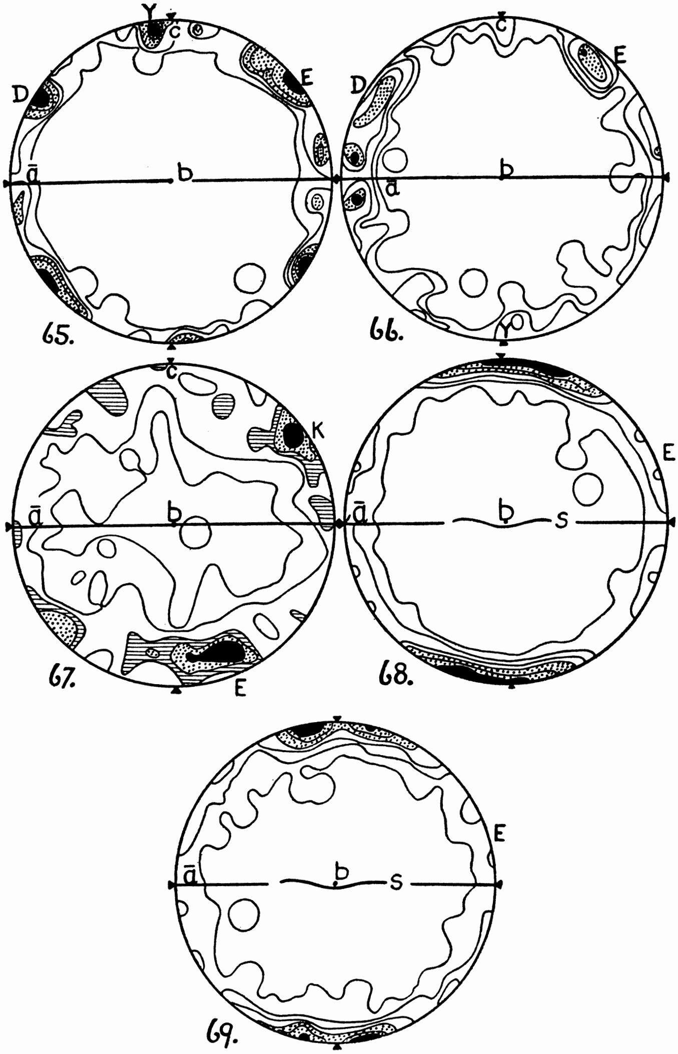

PLATE XI.

Fig. 65. No. 4715, Muscovite, 100 flakes from late-crystallized areas of quartz mica and stilpnomelane. Contours 10, 8, 6, 4, 1%; maximum concentration, 14%.

Fig. 66. No. 4715, Stilpnomelane, 100 flakes from late-crystallized areas of quartz, mica and stilpnomelane. Contours 8, 6, 4, 2, 1%; maximum concentration, 8%.

Fig. 67. No. 4701, Quartz, 330 grains; rotated through 180° about *a*. Contours 4, 3, 2, 1, 0.3%; maximum concentration, 5%.

Fig. 68. No. 4701, Muscovite, 200 flakes; rotated through 180° about *a*. Contours 10, 8, 6, 4, 2, 1%; maxmium concentration, 13%.

Fig. 69. No. 4701, Chlorite, 200 coarse flakes; rotated through 180° about *a*. Contours 10, 8, 6, 4, 2, 1%; maximum concentration, 13%.

constant as evidenced by the centred girdles in the diagrams of all three minerals investigated. The direction of tectonic transport (*a* fabric axis) on the other hand has varied within the plane of deformation *ac*. Within the limits of the measured thin section the traces of the principal visible *s*-surfaces oscillate through a range of 25° on either side of the mean position marked by the megascopic schistosity. Again while the mean position of *a* was approximately parallel to the schistosity during the most important stages of deformation, it assumes a perpendicular position (i.e. it interchanges with the original *c*) during the latest recorded stage when the fabric for quartz, late mica and stilpnomelane was imprinted. The position of *a* shown in all diagrams for this rock is of course the mean *a* for the earlier and most important stages of deformation.

(e) Specimen No. 4715 comes from an outcrop in which the schistosity (*ab*) dips SE at 30°. The strike of the schistosity is N 30° E and makes an angle of 60°-65° with the lineation *b* which has been proved to be the B-axis of the complex deformation deduced from the study of rock fabric discussed above. This divergency between strike of schistosity and trend of the B axis of the mica and quartz fabric seems, from the data at present available, to be a regional condition in the north-eastern portion of the map. The region has therefore been affected by a major movement acting at right angles to a more or less NE-SW axis which is quite unrecorded in the fabric of the measured minerals. This can only have been a late regional tilting of the schistose rocks unaccompanied by any penetrative movement such as would have affected the internal fabric; for it is inconceivable that the intense deformation discussed in this section could have been superposed upon an initially tilted series of schists without causing great complication of their large-scale structure. Further it should be mentioned that whereas the trend of *b* (= B) of the mineral fabric is approximately constant in this area, the pitch of *b* (= B) varies considerably and is always directly related to the dip of the schistosity; this too is strong evidence that an initially subhorizontal *b* (= B) fabric axis of constant trend, corresponding to the trend of *b* (= B) in other parts of the map, has locally been tilted together with the schistosity in which it lies. The late tilting responsible for the inclined attitude of the schists in this northern area must, however, be pre-Cretaceous, for the peneplain cut in these rocks in early and middle Cretaceous time dips regularly seaward at a low angle and therefore bevels the edges of the upturned schists just described (cf. Service, 1933).

Horizontal Schists East of Middlemarch.

Specimen No. 4701

Locality: base of basalt-capped cone about three miles E. of Middlemarch, on road to Macrae's Flat.
Schistosity strongly defined, horizontal, gently curved within limits of hand-specimen.
Lineations: *b*, strike 150°.
b' present only locally, strike 170°.
Joints vertical, strike 70°.

The microstructure is dominated by gently undulating micaceous layers which determine the schistosity and wrap around slender pencils of quartz (lenticular in *ac* section) which have apparently originated by disruption of originally continuous thin layers. The more resistant of the quartzose layers (5-8 mm. in thickness) are less broken and may retain their continuity for several centimeters in the direction of the *a* fabric axis.

The mica of the micaceous bands occurs in sharply defined, easily measured flakes either alone, accompanied by chlorite, or associated with opaque black finely-divided material that is probably magnetite. The orientation of 200 flakes measured in several traverses across the schistosity is shown in Plate XI, Fig. 68—Plate XI, Fig. 69 represents 200 flakes of coarse undeformed chlorite from chlorite-mica bands or aggregates of pure chlorite. The two are closely similar as regards the centred girdle about *b*, strong maximum corresponding to the main *s*-planes and weak paired submaxima at E. The quartz diagram (Plate XI, Fig. 67) was constructed from a plot of 330 poles. It too shows an approximately centred girdle, but the maxima K and E are unrelated to the dominant visible *s*-structure; maximum E does correspond to the weak concentrations at E in the chlorite and mica diagrams, however. This appears to be a clear instance of superposition of a late quartz fabric upon a rock in which the main features of the chlorite and mica fabrics are controlled by subhorizontal slip-surfaces dating from the earlier and main stage of deformation. The tectonic axis *b* remains constant during both stages.

Porphyroblastic Albite-Schists of Waikouaiti River.

In the deeply entrenched valley of the south branch of the Waikouaiti River about three miles west of Merton School, coarse-grained albite-schists with porphyroblasts of albite sometimes reaching 5 mm. in diameter are the dominant rocks (Nos. 4718-4721). The rank of metamorphism attained seems to be higher than in other schists from Central and Eastern Otago, for the place of chlorite is taken by a greenish-brown micaceous mineral which is probably biotite (though possibly a stilpnomelane), and small crystals of garnet are fairly common. Tourmaline is coarser and more plentiful than in other Otago schists known to the writer. The schistosity is distinct and segregation of minerals into bands is roughly developed, but the contorted and ruptured structure typical of the schists described in this paper is lacking in rocks from the present locality. The albite porphyroblasts appear to be a product of static growth and enclose numerous, small crystals of epidote which together with black specks of magnetite dust may build up parallel strings apparently representing an early *s*-structure somewhat oblique to the trace of the schistosity.

Specimens Nos. 4718, 4721

Locality: Northern end of prominent eastward meander. South branch of Waikouaiti River, three miles west of Merton; No. 4718 from great joint-scarp on west side of stream; No. 4721 from outcrop in stream bed 200 yds. further north.

Schistosity, S_1 strikes 20°, with dip of 45° to ESE.[13]

Lineations: *b* (main lineation in No. 4721) trends at 175° with slight pitch to south;
b′ (main lineation in No. 4718, specially marked on quartzose surface) trends at 190°, nearly horizontal.

Joints: regular, strike 30°, dip 45° to NW; strike 120°, vertical, less numerous but very strong, giving rise to prominent scarps many hundreds of yards in length; strike 105°, vertical, rather rare.

Orientation of sections: No. 4718 was cut approximately perpendicular to *b′*; No. 4721, approximately perpendicular to *b*; in both sections an error in cutting has resulted in eccentricity of 5° as indicated in the fabric diagrams.

The dominating feature of the microstructure is a rough banding parallel to the schistosity (S_1) resulting from local

[13] This steep dip is maintained along the northern side of the river, but on the southern side flattens to 10° at a point three-quarters of a mile south and 800 feet higher in altitude than the outcrops here mentioned.

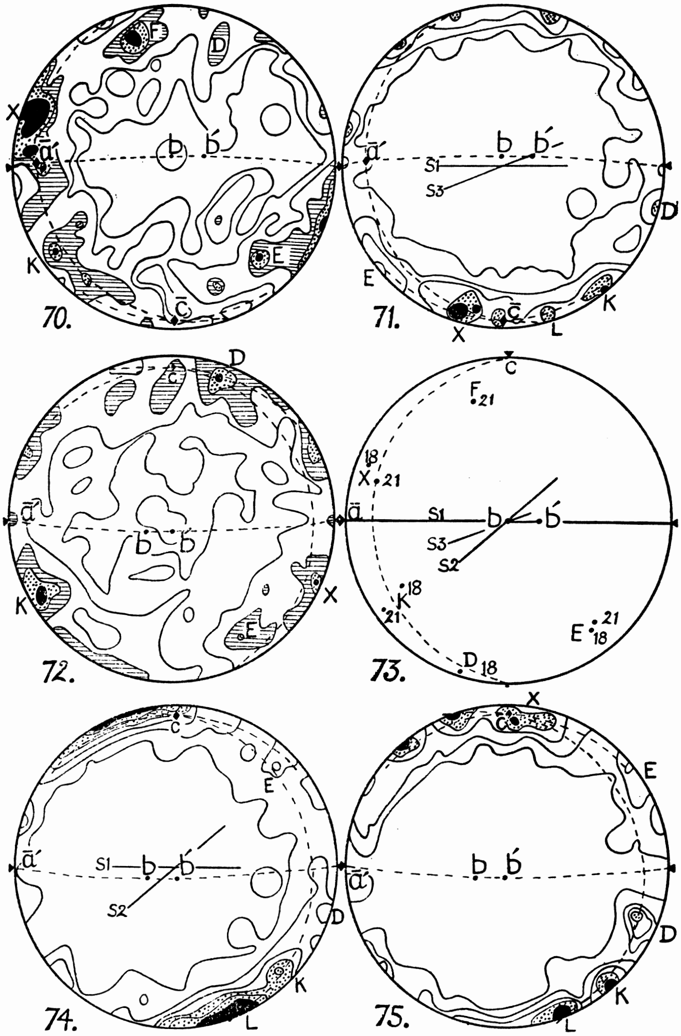

PLATE XII.

Fig. 70. No. 4721, Quartz, 230 grains. Contours 4, 3, 2, 1, 0.5%; maximum concentration, 5%.

Fig. 71. No. 4721, Muscovite, 180 flakes. Contours 8, 6, 4, 2, 0.5%. Traces of S_1 and S_3 are shown.

Fig. 72. No. 4718, Quartz, 400 grains. Contours 4, 3, 2, 1, 0.25%; maximum concentration, 4%.

Fig. 73. Nos. 4718, 4721: Positions of quartz maxima of Figs. 71 and 72, plotted on projection normal to *b*.

Fig. 74. No. 4718, Muscovite, 200 flakes in micaceous layers. Contours 10, 8, 6, 4, 2, 0.5%; maximum concentration, 12%. Traces of S_1 and S_2 are shown.

Fig. 75. No. 4718, Muscovite, 120 flakes in quartzose layers. Contours 8, 6, 4, 2, 0.4%; maximum concentration, 10%.

segregation of quartz, mica or albite combined with a strong tendency for the latter mineral to form porphyroblasts. The trend of the micaceous layers is necessarily flexuous where they pass around the large albites and occasional garnets, but there appear, in addition, to be other *s*-structures, also marked by strings of mica in the *ac* sections, which dip more steeply than the schistosity. These are shown in the diagrams as S_2 (No. 4718) and S_3 (No. 4721), making angles of 35°-42° and 15°-25° respectively with S_1.

The quartz is coarse and clear, with marked undulose banding parallel to the optic axis, and is the main constituent of eyes and discontinuous bands trending parallel to the trace of S_1 as seen in the *ac* section. Superindividuals seem to be present in some of these eyes, necessitating measurement of a large number of grains in order to bring out the general orientation for the rock as a whole. In No. 4721 only 230 grains were available, and the resulting diagram (Plate XII, Fig. 70) is therefore interpreted in conjunction with the corresponding diagram (Plate XII, Fig. 72) for No. 4718 which is based upon 400 grains. In Plate XII, Fig. 73 the principal maxima of Plate XII, Figs. 70 and 72 are replotted after rotation into the *ac* plane perpendicular to *b*. In each case it is clear that the axis of the quartz girdle is *b′*, not *b*, though *b′* is megascopically visible in only one of the two rocks concerned (No. 4718). There is good correspondence between maxima X, E and K, of which the last named is equivalent, perhaps fortuitously, to the mean position of S_2 and S_3 combined. Maximum D, well developed in Plate XII, Fig. 72, is less conspicuous but still clearly indicated by a submaximum in Plate XII, Fig. 70; but a maximum F in Plate XII, Fig. 70 has no counterpart in Plate XII, Fig. 72 and is therefore probably to be attributed to the presence of one or more superindividuals.

The muscovite is unusually coarse and quite undeformed. Plate XII, Fig. 71 (180 flakes) represents total mica encountered in several representative traverses across the schistosity in No. 4721. Plate XII, Figs. 74 (200 flakes) and 75 (120 flakes) are based respectively upon mica of the micaceous bands and the equally coarse but isolated micas enclosed in the quartzose layers and albite porphyroblasts, both as measured in traverses across S_1 in No. 4718. In contrast with the quartz, the mica in each case occupies a girdle whose axis is *b*, not *b′*.

In the total mica diagram, Plate XII, Fig. 71, the poles to (001) are concentrated within a wide arc extending on both sides of the pole of S_1. The spread of maxima and submaxima through this arc might be the result of undulation of a single set of *s*-surfaces, or alternatively might indicate the existence of several sets of *s*-surfaces intersecting at low angles. The second alternative is supported by development of

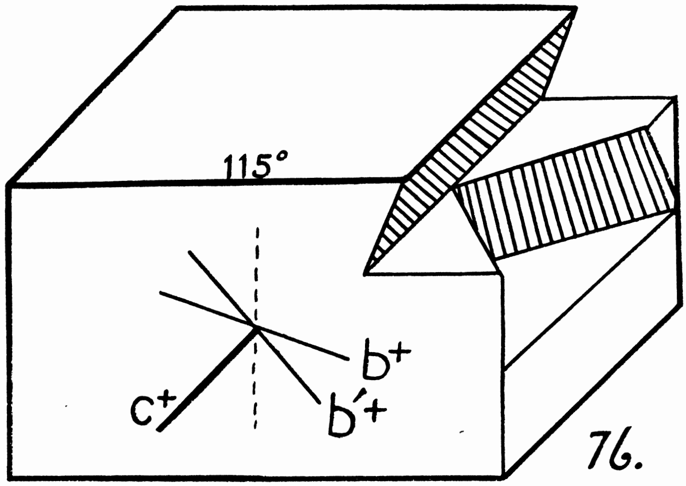

Fig. 76. No. 4726, Ideal sketch of hand-specimen showing macroscopically observable structures. Front face of block is southern schistosity surface with strike (115°) horizontal. Main joint surfaces shaded.

closely corresponding maxima L, K, and submaxima D, E, in Plate XII, Fig. 74, and in the writer's opinion is conclusively proved by the presence in Plate XII, Fig. 75 of exactly equivalent maxima. Undulation of a single set of *s*-surfaces around lenses of quartz and coarse albites cannot be responsible for the spread of maxima in Plate XII, Fig. 75, since the mica in question occurs as isolated flakes within the quartz and albite.

From the mica diagrams it would appear that the megascopic schistosity S_1 is determined by the roughly laminated condition of the rock, accentuated by the tendency for some of the mica to lie subparallel to S_1, especially that enclosed in the quartz. More important in their influence on the mica fabric are S_2 and S_3 (maxima K and L) which are clearly separate identities although not both visible in every thin section. A fair degree of correspondence between the quartz and mica maxima is evident especially in the case of points X and D, suggesting that the quartz fabric has been influenced to some extent by *s*-surfaces parallel to which the micas have also crystallized. In contrast with this, however, the lack of coincidence of the girdles for mica and quartz respectively accords with the writer's view that in general, deformation took place in at least two distinct stages.

Finally attention is drawn to the steeply inclined attitude of the schistosity, the strike of which is inclined at only 10° to the axis of the quartz girdle. Fabric analyses of other rocks must be carried out before it can be decided if tilting of the schistose rocks were subsequent to or contemporaneous with the imprint of the quartz fabric upon the rock. It may be pointed out, however, that the quartz diagrams (especially that for No. 4718, Plate XII, Fig. 72) agree well with that for No. 4715 (Plate X, Fig. 59) when the megascopic schistosity is taken as datum for comparison, and in this latter instance tilting was apparently later than development of the quartz fabric.

Vertical Schists From Local Fault-Zone, Lee Stream.

Where the Hindon-Outram road crosses Lee Stream below Mt. Hyde, the schists locally assume a vertical attitude in a fault zone exposed for a distance of 100 ft. or more in road-cuts on the north bank of the river. Two rocks collected from the middle of this zone (Nos. 4725, 4726) are both strongly lineated in two directions which pitch eastward at 20° and 50° respectively. If the hand-specimen is rotated about the line of strike (115°) so as to bring the southern surface into the top horizontal position, the strikes of the lineations are 135° and 165° respectively (cf. Fig. 76). These directions agree with the major and minor lineations observed in adjacent horizontally disposed rocks (Nos. 4722-4724), and it is therefore safe to assume that the schists of the fault-zone have been vertically tilted or slightly overturned so that the originally upper surfaces now face towards the south.

The following structural details of the faulted and adjacent schists are recorded:

(a) South rim of gorge, one mile distant from and about 800 ft. higher than the outcrop of the fault.

Schistosity horizontal.
Lineation, 145°.
Vertical joints strike 60°.

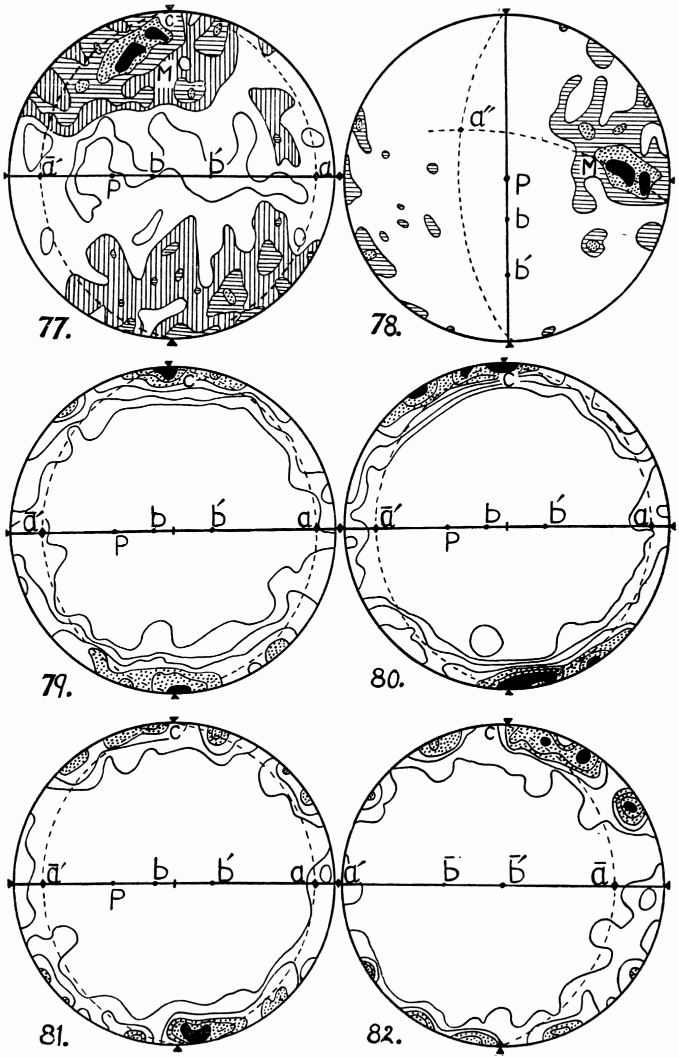

PLATE XIII.

Fig. 77. No. 4726, Quartz, 400 grains. Contours 4, 3, 2, 1, 0.5%; maximum concentration, 5%. p = pole of strike of schistosity-surface *ab*.

Fig. 78. Quartz diagram Fig. 77 rotated through 30° about *c* to bring the pole (p) of the strike of the schistosity surface into the centre of the projection. Schistosity dips vertically. Contours 4, 3, 2%.

Fig. 79. No. 4726, Chlorite, 150 flakes. Contours 10, 8, 6, 4, 2, 0.7%; maximum concentration, 11%.

Fig. 80. No. 4726, Muscovite, 100 flakes in mica-chlorite layers. Contours 10, 8, 6, 4, 2, 1%; maximum concentration, 12%.

Fig. 81. No. 4726, Muscovite, 80 long slender flakes enclosed in quartzose portion of section. Contours 10, 8, 6, 4, 1%; maximum concentration, 10%.

Fig. 82. No. 4725, Muscovite, 100 flakes. Contours 10, 8, 6, 4, 1%; maximum concentration, 12%. (Note that this diagram is in reverse position to the others; i.e., the fabric is seen from the SE (positive) end of *b* instead of from the NW (negative) end).

(b) South bank of Lee Stream 200 yds. from outcrop of fault.

Schistosity strikes 155°, dip 25° to NE.
Lineation 140°.
Steep joints strike 45°-55°, 75°.

(c) In fault-zone itself (Nos. 4725, 4726).

Schistosity strikes 115°, dip 80°-90° to N.
Lineations in schistosity-planes pitch eastward at 20° (b) and 50° (b'); faint vertical lineation locally present.
Joints rather irregular: strike 15°-35° with steep dip to W; strike 75° with dip 70° to N (cf. Fig. 76).

Specimen No. 4726

Orientation: schistosity plane = ab; lineation with 20° pitch = b (east end positive); normal to southern surface of schistosity = positive end of c; thin section for fabric analysis cut at an angle of 80° to the negative end of b and perpendicularly to ab.

Quartz is the main constituent of lenticular aggregates and discontinuous layers alined subparallel to the schistosity. Relatively coarse, usually undulose grains have been granulated at the margins and are set in a matrix of fine-grained quartz. Plate XIII, Figs. 77 and 78 are based upon 400 measurements, including grains of all types. These diagrams differ from those previously described in this paper in that there is a strongly developed point maximum M, and a minimal belt coinciding with the trace of ab, while the usual girdle pattern is only faintly indicated. It is assumed that these unusual features are the expression of late penetrative movement connected with the local faulting, a view which is supported by the granulated condition of much of the quartz. The maximum M is unrelated to the schistosity and according to current interpretation indicates movement in a single set of slip-surfaces, the quartz being oriented with either $(10\bar{1}0)$ or (0001) in the plane of slip. If the first of these alternatives held, the corresponding direction of movement would have been almost perpendicular to the schistosity, a condition difficult to picture in a fault-zone of this type. It is more likely that the orientation of the quartz is governed by movement on the basal plane, in which case the dotted vertical arc of Plate XIII, Fig. 78, representing the plane perpendicular to M would be the plane ($a''b''$) in which the late movement occurred. Any attempt to fix the a''

and *b″* directions within this plane is speculative, but some indication is afforded by the direction in which the principal maximum is elongated. If the elongated maximum is the first stage in development of a girdle about *b″*, then the direction of movement *a″* is given approximately by drawing a great circle along the line of elongation of maximum M (Plate XIII, Fig. 78). As a hypothesis to explain the quartz orientation in No. 4726, the writer therefore suggests that the main factor responsible was late movement in a direction *a″* (pitching westward at about 35°) in a vertical plane (vertical arc of Plate XIII, Fig. 78) inclined at 25° to the schistosity. The faint third lineation observed at 90° to the strike of the schistosity could represent the intersection of the schistosity-surfaces with these planes of late slip. If, as is probable from analogy with adjacent rocks, the quartz grains had earlier assumed an orientation with the poles of the optic axes concentrated in an arc centred about the *c* fabric axis in the earlier main deformation, many grains would have been in a favourable position to glide later on (0001) in the manner suggested above.

Three diagrams were prepared for mica and chlorite in No. 4726: Plate XIII, Fig. 79 based on 150 flakes of chlorite, mainly in mica-chlorite bands; Plate XIII, Figs. 80 and 81 representing clear-cut, undeformed mica in mica-chlorite bands (100 flakes) and quartzose bands (80 flakes) respectively. All three are closely similar in showing a good girdle centred about an axis between *b* and *b′*, a strong maximum corresponding to the pole of the schistosity and other maxima in mutually comparable positions. The position of the axis of mica and chlorite girdles (intermediate between *b* and *b′*) was verified by construction of another mica diagram (Plate XIII, Fig. 82) based on 100 flakes in an *ac* section of No. 4725. In this and other respects the mica and chlorite diagrams are closely comparable with those for rocks outside the fault zone (e.g. Plate II, Figs. 8, 9, Plate III, Figs. 14, 18, etc.), so that mica and chlorite have been almost unaffected by the movements involved in the faulting. This is borne out too by the complete lack of relation between the chlorite-mica and the quartz fabrics.

SUMMARY OF TECTONIC HISTORY OF EASTERN OTAGO.

In conclusion, the writer's conception of the complex tectonic history of eastern Otago, in the light of structural features discussed in this paper or recorded by other writers, is presented in outline. It will be obvious that the relative order of some of the events recorded in the rock structures is still uncertain, while others may yet remain undetected.

(1) The earliest stage of deformation clearly recorded is that connected with the main phase of metamorphism. Rocks of greywacke composition were reduced to a phyllonitic condition by intense penetrative movement on slip-surfaces that were for the most part gently inclined or horizontal. Subsequent mineralogical reconstitution, accompanied by segregation of particular minerals into subparallel bands, was followed by renewed deformation involving slip on the old schistosity surfaces, contortion of the segregation-bands and even disruption of the competent quartzose layers into separate pencils, and in some rocks initiation of new schistosity surfaces as planes of slip cutting across the older *s*-planes. The end-products were rocks with nearly horizontal or locally steeply inclined schistosity, and prominent subhorizontal lineation (*b*) which is the tectonic axis (NW to NNW). In some rocks the schistosity was obscured by the presence of several intersecting *s*-surfaces or by intense micro-folding and disruption of the component laminae, but in such rocks the lineation is correspondingly stronger.

(2) A second lineation b' with a consistently more northerly trend (NNW to N) than *b* is ascribed to a subsequent movement of slip in the surfaces of schistosity in a direction approximately perpendicular to b'. This same movement is believed to be responsible for the slight eccentricity with respect to *b*, displayed by the girdles for mica, chlorite, and stilpnomelane in most rocks.

(3) Still later the main features of the quartz fabric have been imprinted. The tectonic axis, as indicated by the axis of the quartz girdle, now trends NW or in a few instances N, and usually diverges distinctly from *b* and b' of stages (1) and (2) respectively. Movement now appears to have been concentrated on (but not confined to) steeply inclined surfaces of slip, indicating that the strong lateral displacement of the earlier deformation had given place to subhorizontal compression without noteworthy displacement. The mica and chlorite fabrics have been slightly affected by these movements.

(4) Throughout the northeast portion of the map, the schists have been tilted across a general NE-NNE strike so that they now dip at angles of 12°-30° or locally even more

steeply. This tilting is later than the imprint of the quartz fabric but precedes the peneplanation that occurred during the earlier part of Cretaceous time. Probably some of the post-metamorphic faulting observed elsewhere, e.g. in the gorge of Lee Stream, belongs to this period, though in the instance cited, the strike of the faulted beds is WNW.

(5) Block-faulting with a constant NE trend, often involving displacements of several thousand feet, has been active throughout Eastern and Central Otago during the late Tertiary but has not affected the rock fabrics except in the immediate vicinity of the fault-planes (specimens have not yet been subjected to fabric analyses).

At several localities within or bordering upon the area here discussed, notably at Macrae's Flat, Nenthorn, Oturehua, Waipori, and Saddle Hill, auriferous quartz lodes cut the schists of the Maniototo series (Marshall, 1918, pp. 37-41; Grange, 1921; Williamson, 1934, pp. 8, 9). These must be at least as old as early Cretaceous, for derived gold is present in the late Cretaceous and Tertiary gravels that lie upon the peneplain cut in the basement schists. Most of the gold-bearing veins strike NW and dip steeply across the schistosity, and in these respects resemble the slip-planes that are believed to have controlled development of the quartz fabric in the schists themselves. It is clear, therefore, that the auriferous lodes were deposited during the later stages of metamorphism, probably along surfaces determined during stage (3) as defined above (cf. Williamson, 1934a, p. 119).

The present investigation sheds little new light upon the vexed question of the possible relation between metamorphism in the schist area of Otago and the great orogeny during which the flanking Triassic and Jurassic rocks were folded late in the Jurassic. Some part or the whole of the sequence of events described under (1)-(3) above must be ascribed to this orogeny. The present writer's view, based upon considerations outside the scope of this paper, that the main metamorphism of stage (1) was accomplished before the middle of the Triassic, receives slight additional support in the complexity of the sequence of events that certainly was completed prior to the peneplanation that followed upon the late Jurassic orogeny. The general northwest trend of the folded Mesozoic rocks north and south of the schist area would agree almost equally well with the mean trends of the two usual lineations or the axis of the quartz girdles.

ACKNOWLEDGMENTS.

This investigation has been carried out under the direction of Professor and Mrs. Adolph Knopf during tenure of a Sterling Fellowship at Yale University. I wish to acknowledge my indebtedness to the Corporation of Yale University who have thus made the work possible; to Professor Bruno Sander of Innsbruck University who gave critical advice as to procedure, and especially to Professor and Mrs. Knopf for frequently given advice and helpful suggestions, and for reading and criticism of the manuscript prior to publication. Though taking full responsibility for the results here presented, I gratefully record the benefit received from discussion of procedure and results with Mrs. Knopf at every stage of the investigation.

LITERATURE CITED.

Fairbairn, H. W.: Hypotheses of Quartz Orientation in Tectonites. Bull. Geol. Soc. Amer., Vol. 50, pp. 1475-1492, 1939.

Finlayson, A. M.: Some Observations on the Schists of Central Otago. Trans. N. Z. Inst., Vol. 40, pp. 72-79, 1908.

Grange, L. I.: The Geology of the Green Island Coalfield. Trans. N. Z. Inst., Vol. 53, pp. 157-174, 1921.

Griggs, D., and Bell, J. F.: Experiments bearing on the Orientation of Quartz in Deformed Rocks. Bull. Geol. Soc. Amer., Vol. 49, pp. 1723-1746, 1938.

Knopf, E. B.: Retrogressive Metamorphism and Phyllonitization. This Journal, Vol. 11, p. 1-27, 1931.

Mackie, J. B.: A Geological Traverse from the Waitaki River to Dunstan Peak, Otago. Trans. Roy. Soc. N. Z., Vol. 66, Pt. 2, pp. 125-142, 1936.

Marshall, P.: The Geology of the Tuapeka District. N. Z. Geol. Surv. Bull., No. 19, 1918.

Sander, B.: Gefügekunde der Gesteine. J. Springer, Vienna, 1930.

Schmidt, W.: Tektonik und Verformungslehre. Borntraeger, Berlin, 1932.

Service, H.: The Geology of the Goodwood District, North-east Otago, New Zealand. N. Z. Jour. Sci. and Tech., Vol. 15, pp. 263-279, 1933.

Turner, F. J.: Metamorphism of the Te Anau Series in the Region Northwest of Lake Wakatipu. Trans. Roy. Soc. N. Z., Vol. 65, Pt. 3, pp. 329-349, 1935.

———: Interpretation of Schistosity in the Rocks of Otago, New Zealand. Trans. Roy. Soc. N. Z., Vol. 66, Pt. 2, pp. 201-224, 1936.

———: Progressive Regional Metamorphism in Southern New Zealand. Geol. Mag., Vol. lxxv, pp. 160-174, 1938.

———: Petrofabric Investigations of Otago Schists, No. 2. Trans. Roy. Soc. N. Z., Vol. 68, Pt. 1, pp. 107-121, 1938 (a).

Williamson, J.: Naseby Subdivision. Ann. Rept. N. Z. Geol. Surv., No. 28, pp. 6-10, 1934.

———: Quartz Lodes of Oturehua, Nenthorn and Macrae's Flat, Otago. N. Z. Jour Sci. and Tech., Vol. 16, pp. 102-120, 1934 (a).

UNIVERSITY OF OTAGO,
DUNEDIN,
NEW ZEALAND.